Manuscript prepared for Atmos. Meas. Tech.
with version 2014/07/29 7.12 Copernicus papers of the LaTeX class copernicus.cls.
Date: 15 April 2019

Trends in the atmospheric water vapour estimated from GPS data acquired in Sweden and Finland and analyzed using different elevation cutoff angles

Tong Ning[1] and Gunnar Elgered[2]

[1]Lantmäteriet (The Swedish Mapping, Cadastral and Land Registration Authority), SE-80182, Gävle, Sweden
[2]Department of Space, Earth and Environment, Chalmers University of Technology, Onsala Space Observatory, SE-43992 Onsala, Sweden.

Correspondence to: T. Ning (tong.ning@lm.se)

Abstract. We have processed 20 years of GPS data from 8 sites in Sweden and 5 sites in Finland, using two different elevation cutoff angles 10° and 25°, to estimate the atmospheric integrated water vapour (IWV). One additional parameter has also been tested in the GPS data processing, i.e., with or without elevation dependent data weighting. We estimated the IWV trends for GPS solutions with the elevation cutoff angles of 10° and 25° under three scenarios, i.e., (1) no corrections for interventions, (2) corrections carried out for known interventions, and (3) corrections also carried out for interventions detected for unknown reasons, by a PMTred test, for the GPS 10° solution. Thereafter, we compared the GPS-derived IWV trends to the corresponding trends from radiosonde data at 7 nearby ($<$ 120 km) sites and the trends inferred from the European Centre for Medium-Range Weather Forecasts (ECMWF) reanalysis data (ERA-Interim). As expected the lowest correlation ($<$ 0.6) is obtained when the trends from the nearby radiosonde data and the ERA-Interim data were compared to the IWV trends given by the GPS data without corrections for the interventions. The trend agreement is significantly improved when the GPS data were corrected for both known as well as unknown interventions. Furthermore the best agreement of the trends between two GPS solutions was given by the scenario (3) with a correlation coefficient of 0.91. The trends obtained from the GPS 10° solution with a data weighting show no significant differences when compared to radiosonde and ERA-Interim data while the agreement becomes worse for the GPS 25° solution. The results indicate that the use of different elevation cutoff angles in the GPS data processing is a valuable diagnostic tool for detection of any time varying systematic effects, such as signal multipath.

1 Introduction

Atmospheric water vapour is a very important greenhouse gas due to its ability of absorbing long wave thermal radiation emitted from the Earth's surface. A warmer climate increases the amount of water vapour, which further reduce the amount of long-wave radiation escaping from the Earth to space, and thereby leading to an even warmer climate. Hence, the atmospheric water vapour is one of the most significant climate feedback processes and atmospheric integrated water vapour (IWV) can be used as an independent data source for monitoring climate changes. This, however, requires accurate observations with a long-term stability in order to have a high accuracy of the estimated trends in the IWV. With a relatively high temporal resolution, continuously improving spatial density, and less expensive receivers, ground-based GNSS networks have been identified as a useful technique to obtain long-term trends in the atmospheric IWV [e.g., *Wang et al*. 2007, *Nilsson and Elgered* 2008, and *Vey et al*. 2010].

A reliable estimate of the IWV trend requires homogeneous input data. The observations acquired from the ground-based GNSS sites may, however, contain interventions which need to be thoroughly investigated and corrected, if it is possible, before GNSS-derived IWV are used for climate monitoring. *Ning et al.* (2016a) pointed out that these are mainly due to systematic errors and cannot be averaged out as the time series of the measurements becomes longer. The origin of these errors can either be related to data processing, hardware changes, or the electromagnetic environment at the antenna site (*Vey et al.*, 2009). The first type of errors can be significantly reduced after a homogenous data reprocessing over the whole time series (*Steigenberger et al.*, 2007). Hardware changes are normally well documented. For example, for most of the continuously operating GNSS sites, e.g., in the International GNSS Service (IGS) network (http://www.igs.org) and the Tide Gauge Benchmark Monitoring (TIGA) project (*Schöne et al.*, 2009), there are archived log files with a common format to record all hardware changes. This is normally done by the owners of the GNSS sites, where a continuously updated log file for each site is provided (*Ning et al.*, 2016b). Such log files are very important for the future homogenization of the data.

Changes in the electromagnetic environment result in different multipath effects on the GNSS observations. In difference to the hardware changes, which typically result in an instant constant offset, the interventions caused by multipath effects are normally not fixed in time but varies with the reflective properties, e.g., growing vegetation (*Pierdicca et al.*, 2014) and/or different soil moisture (*Larson et al.*, 2010). Such slowly varying changes are very difficult to quantify. After examination of 19 years of data obtained at 101 TIGA sites, *Ning et al.* (2016b) found that about 70 % of the detected interventions in the GNSS-derived IWV time series cannot be related to any documented hardware change. Some of these detections may be false but the interventions in the IWV time series induced by multipath effects need to be eliminated, or at least significantly reduced.

In GNSS data processing, low elevation angles are used in order to improve the geometry which reduces the formal error of the individual IWV estimate. This is an advantage when we use the

inferred IWV for validation of specific observations over short time scales or in forecasting applications. For example, the ground-based GNSS IWV was identified as a priority one measurement for GCOS (Global Climate Observing System) Reference Upper Air Network (GRUAN) (*Ning et al.*, 2016a). However, if we use the IWV estimates for monitoring the long-term changes in the atmospheric water vapour, e.g., as linear trends, the formal error of the individual IWV is not the limiting factor (*Nilsson and Elgered*, 2008). In this case, the homogeneity of the IWV time series is more important where higher elevation cutoff angles may be desired if signal multipath effects cannot be modelled accurately for observations at low elevation angles. Using 14 years of GPS data from 12 sites in Sweden and Finland, *Ning and Elgered* (2012) found that a higher elevation cutoff angle (25°) gave the best agreement between the GPS-derived IWV trends and the ones obtained from radiosonde profiles at nearby launching sites. *Baldysz et al.* (2018) estimated IWV for a time period of 20 years (1996-2015) using the data acquired from 20 GPS sites in the EUREF Permanent Network (EPN). They found a better agreement with nearby radiosonde-derived IWV trends for the 20° elevation cutoff solution when compared to a 5° solution.

In GNSS data processing an elevation-dependent data weighting is sometimes used. It is actually recommended for the data processing of the EUREF permanent network (*Huber and Kaniuth*, 2003). When the elevation cutoff angle is lower than 20°, *Huber and Kaniuth* (2003) found better repeatabilities of the daily north and east position components, over an analysed time period of ten days, after applying elevation-dependent weighting functions in the GPS data processing. We know that elevation-dependent errors, e.g., multipath effects, may introduce systematic errors in terms of biases. When studying trends the question is if these biases vary over these long time scales and thereby affecting the accuracy of estimated trends. Therefore, it is of great interest to investigate if the implementation of elevation-dependent data weighting in combination with different cutoff angles in the GPS data processing can reduce the impact of such systematic errors on the resulting IWV trends.

We carried out a study with a focus on the elevation-angle-dependent parameters and their corresponding impacts on the resulting IWV linear trends. Compared to the work by *Ning and Elgered* (2012) the time series are 20 years instead of 14 years, and the IWV estimated from the GPS data are now also compared to ERA-Interim data in addition to the radiosonde data. In addition, now the concept of elevation dependent data weighting and the impact of corrections for interventions in the GPS IWV time series are also studied. The data sets are described in Section 2 where details about the GPS data processing are given. The primary interest of this work is if there are multipath, or other antenna environment, effects on the estimated IWV. Therefore we need to assess the GPS observations for known (documented) interventions, e.g., due to hardware changes, and unknown (undocumented) interventions, e.g., due to multipath effects. This is discussed in Section 3 which also gives details on the estimation of IWV trends. Section 4 presents the comparisons of the GNSS-

derived IWV with the ones obtained from the different data sets. Finally, the conclusions are given in Section 5.

2 Data sets

2.1 GPS

We have analysed 20 years (from 1 January 1997 to 31 December 2016) of ground-based GPS observations acquired from 8 sites in the Swedish reference network (SWEPOS) and 5 sites in the Finnish reference network (FinnRef). Figure 1 depicts the location of the sites and their coordinates are given in Table 1.

A standard data processing was carried out using GIPSY/OASIS II v.6.2 (*Webb and Zumberge*, 1993) with the Precise Point Positioning (PPP) strategy (*Zumberge et al.*, 1997). The inputs of the processing were ionospheric free linear combinations formed by acquired GPS phase-delay observations while the output included station coordinates, clock biases, and tropospheric parameters. The final GPS orbit and clock products used were provided by Jet Propulsion Laboratory (http://gipsy.oasis.jpl.nasa.gov/gipsy/docs/GipsyUsersAGU2007.pdf). An ocean tide loading correction using the FES2004 model (*Lyard et al.*, 2006) was applied while no atmospheric pressure loading corrections were used. The absolute calibration of the Phase Centre Variations (PCV) for all antennas (from the file igs08_1869.atx) was implemented (*Schmid et al.*, 2007) and the technique of ambiguity resolution was applied (*Bertiger et al.*, 2010).

The ZTD and linear horizontal gradients were estimated using a random walk model with a standard deviation (SD) of 10 mm/$\sqrt{\mathrm{h}}$ and 0.3 mm/$\sqrt{\mathrm{h}}$, respectively. The SD value used for the ZTD is given by *Jarlemark et al.* (1998) where they found a temporal variability in the wet delay, derived from 71 days of microwave radiometer measurements, varying in the interval 3–22 mm/$\sqrt{\mathrm{h}}$ at the Onsala site. This value however is larger than the one given by http://acc.igs.org/workshop2016/presentations/Plenary_05_03.pdf where they recommend a SD value of 3 mm/$\sqrt{\mathrm{h}}$ when applying an equal weighting. In order to investigate possible impacts of using a larger SD value on the resulting IWV trends we have processed data again for two sites (SODA and OVE0) which are located far north (expecting a less variability of the wet delay) using a random walk model with a SD of 3 mm/$\sqrt{\mathrm{h}}$. The result indicates an insignificant difference (< 0.05 kg/(m^2·decade)) in IWV trends. Therefore in order to be able to capture any large variations of the water vapour we decided to use the large value of SD (10 mm/$\sqrt{\mathrm{h}}$) for all 13 sites.

The ZTD estimates were updated every 5 min using the Vienna Mapping Function 1 (VMF1) (*Boehm et al.*, 2006). They were then averaged using a time window of $\pm$ 0.5 h to have a temporal resolution of 1 h, and converted to the IWV using the following procedure (*Ning et al.*, 2016a).

The ZTD is the sum of the Zenith Hydrostatic Delay (ZHD) and the Zenith Wet Delay (ZWD).

$$\ell_t^z = \ell_h^z + \ell_w^z \tag{1}$$

The ZHD for a given GPS site can be calculated (*Saastamoinen*, 1973):

$$\ell_h^z = \frac{2.2767 \cdot P_0}{f(\lambda, H)} \tag{2}$$

where P_0 is the ground pressure in hPa and

$$f(\lambda, H) = \left(1 - 2.66 \cdot 10^{-3} \cos(2\lambda) - 2.8 \cdot 10^{-7} H\right) \tag{3}$$

determined by λ and H which are the site latitude and the height above the geoid in m, respectively.

The ZWD is related to the IWV via the conversion factor Q (*Ding*, 2018)

$$V = \frac{\ell_w^z}{Q} \tag{4}$$

where Q is defined by

$$Q = 10^{-6} \rho_w R_w \left(k_2' + \frac{k_3}{T_m}\right) \tag{5}$$

where ρ_w is the density of liquid water; R_w is the specific gas constant for water vapour; k_3 and k_2' are two constants which can be estimated from laboratory experiments; T_m is a mean temperature, weighted by the wet refractivity, in units of K.

The standard data processing was first performed twice using two different elevation cutoff angles (10° and 25°). Thereafter we processed the data for all 13 GPS sites again with an elevation dependent weighting function for both elevation cutoff angles. The weighting function applied was $W = \sin(E)$ where E is the elevation angle.

2.2 Radiosonde

Measurements from 7 radiosonde sites (see Figure 1) were obtained from the database provided by National Oceanic and Atmospheric Administration (NOAA) (https://ruc.noaa.gov/raobs/). As seen in Table 1, the maximum distance between the GPS site and the corresponding nearby radiosonde site is around 120 km while the height difference is less than 100 m for most of the paired sites. The radiosonde data consist of vertical profiles of pressure, temperature, and humidity. The standard vertical levels in radiosonde observations are 1000, 925, 850, 700, 500, 400, 300, 250, 200, 150, 100, 70, 50, 30, 20, and 10 hPa (*WMO*, 1996). We linearly interpolated these profiles up to 12 km at intervals of 50 m, and integrated the absolute humidity in order to calculate the IWV.

Radiosondes are at the most launched four times per day (but more common is two times per day) and the profiles are reported at the nominal time epochs 0:00, 6:00, 12:00, and 18:00 UTC. Figure 2 depicts the number of radiosonde observations obtained from each site for every year. It is clear that the launch frequency of radiosondes has changed significantly over the years. For example we note that four sites (Sundsvall, Jokioinen, Jyväskylä, and Sodankylä) have more frequent launches over the years from 2011 to 2014 while the number of launches for two sites (Landvetter and Luleå) decreases significantly over the last 10 years.

The radiosonde data have been validated by *Ning et al.* (2012) where they presented comparisons of 10-year-long time series of the atmospheric ZWD, estimated using GPS, geodetic very long baseline interferometry (VLBI), a water vapour radiometer (WVR), radiosonde observations, and the ERA-Interim for the IGS site ONSA. We note that all radiosonde sites used in this work changed the type of humidity sensor (from RS80 to RS92) late in 2005 and early in 2006. *Ning and Elgered* (2012) pointed out that since the offset due to the change of instrument will alias with the offset due to different weather conditions before and after the occurrence of change, it is very difficult to perform a reliable correction on the radiosonde-derived IWV. Meanwhile, *Ning and Elgered* (2012) found that due to similar occurrence date of changes for all radiosonde sites in the investigated region (Sweden and Finland), neglect of the offset corrections on radiosonde data resulted in insignificant impacts on the correlation coefficients between the IWV trends from the radiosonde and the GPS data. Furthermore, the expected small offset in the IWV due to the height difference between the GPS and the radiosonde sites (see Table 1) has no significant impact in the trend values.

The radiosonde data obtained from NOAA, for the site of Sodankylä, were also validated using the GRUAN corrected data where algorithms were developed to correct systematic errors in RS92 data and to derive an uncertainty estimate for each data point and each parameter (*Dirksen et al.*, 2014). Using the data covering the time period from 2011 to 2016, we found a mean IWV difference of 0.95 kg/m^2 with a standard deviation of 0.31 kg/m^2. In addition we estimated the trend in the difference between the GRUAN and the NOAA data which shows an insignificant value of 0.0021 kg/(m^2·decade).

Based on the discussion above and concerning the fact that potential offsets will have insignificant impacts on the differences in the resulting trends between the different elevation cutoff angles, we decided not to try to correct for any offsets in the radiosonde data.

2.3 ERA-Interim data

ERA-Interim, the reanalysis product by ECMWF, provides the IWV time series with a temporal resolution of 6 h and a horizontal resolution of about 80 km. It has 60 vertical levels in a range from 0.01 km to 64.56 km (*Berrisford et al.*, 2011). For ERA-Interim, data acquired from many observing systems (i.e., numerous satellite instruments, radiosondes, buoys, and other components) were assimilated. Even though radiosonde data are a fraction of the data assimilated into ERA-Interim, there are still many other observing systems contributing to the data. Therefore we use ERA-Interim data as the other reference data for the IWV comparisons with GPS data.

The ERA-Interim IWV were first interpolated horizontally to the GPS site using the ECMWF interpolation library (EMOSLIB, http://www.ecmwf.int) and details about the horizontal interpolation are given in (https://confluence.ecmwf.int/display/EMOS/Grid+point+to+Grid+point+Interpolation). In this work, since we use the ground pressure and mean temperature obtained from ERA-Interim for the conversion between ZTD and IWV for the GPS data, it is necessary to reduce the difference

between the model height and the GPS antenna height. We carried out a vertical interpolation of the ERA-Interim data to the height of the GPS antenna as follows (*Heise et al.*, 2009). If the GPS height is above the lowest ERA-Interim level, the temperature and specific humidity were linearly interpolated while pressure was logarithmically interpolated to the GPS height. If the GPS site is below the lowest level in ERA-Interim, the temperature was extrapolated using the mean temperature gradient of the three lowest layers. The pressure was calculated by stepwise application of the barometric height formula for each 20 m while the specific humidity is estimated in parallel assuming that the mean relative humidity of the two lowest ERA-Interim levels is representative for the atmosphere below. Finally a linear temporal interpolation of the ERA-Interim data was applied to have the same temporal resolution as in the IWV time series from the GPS data (1 h).

The ERA-Interim product has been evaluated in other studies. Using ground-based GPS measurements acquired from the EUREF Permanent Network (EPN, http://www.epncb.oma.be, each with a maximum time series of 18 years, *Pacione et al.* (2017) produced a ZTD product from the second reprocessing campaign of the EPN (Repro 2). The comparison between the GPS and ERA-Interim data gave a mean ZTD difference of 1.8 mm (0.26 kg/m^2 in IWV) and a standard deviation of 7.8 mm (1.2 kg/m^2 in IWV). The linear IWV trends estimated from the ERA-Interim data were investigated by *Bock et al.* (2014) and were compared to the ones obtained from Doppler Orbitography Radiopositioning Integrated by Satellite (DORIS) measurements at 81 global sites. The ERA-Interim data compared to the homogenized DORIS data resulted in a correlation coefficient which is larger than 0.95. A more recent study, *Parracho et al.* (2018) investigated IWV trends from two reanalyses (ERA-Interim and MERRA-2) from 1980 to 2016. The result showed consistent trends in ERA-Interim and MERRA-2, with positive IWV trends generally correlated with surface warming.

3 Data analysis

3.1 Trend estimation

Linear trends of the IWV were estimated by using a model with annual and semi-annual terms (details are described by *Nilsson and Elgered* (2008)):

$$y = y_0 + a_1 t + a_2 \sin(2\pi t) + a_3 \cos(2\pi t) + a_4 \sin(4\pi t) + a_5 \cos(4\pi t) \quad (6)$$

where y and t are the IWV and the time in years (from 1 January 1997 at UTC 0:00), respectively. The parameters y_0 and a_1 are a constant and a linear trend, respectively; a_2 and a_3 are annual component coefficients, and a_4 and a_5 are semi-annual component coefficients. All unknown coefficients are determined using the method of least squares.

In order to avoid possible differences in the estimated IWV trends due to different sampling intervals of the different techniques, a data synchronization is necessary. This was done by using only the

GPS and the ERA-Interim data acquired, from the very same hour, as the launches of the radiosondes.

For the GPS data the trend estimations were carried out under three scenarios. (1) The IWV trends were first estimated using the GPS data without any corrections. (2) We estimated IWV again after the corrections, for both 10° and 25° solutions, for the known interventions which are supported by the documentation (discussed in Section 3.2.1). (3) A further correction was performed on the GPS 10° solution for interventions detected for unknown reasons, by a PMTred test (discussed in Section 3.2.2). The IWV trends for the GPS 10° solution were estimated once again after the correction.

3.2 Interventions in GPS IWV time series

3.2.1 Known interventions

There are in total 7 GPS sites which have interventions due to known hardware changes over the investigated time period. These changes are listed in Table 2. Most of the interventions are due to antenna changes while three are due to radome changes. One intervention at the site SPT0 is caused by adding microwave absorbing material to the antenna. The offset caused by each intervention was estimated as the mean difference in the GPS and ERA-Interim IWV difference time series before and after the occurrence of the intervention. All estimated mean differences are also presented in Table 2 with the values varying from -1.40 to $+1.78$ kg/m^2.

Figure 3 depicts the time series of daily mean IWV difference between the GPS and ERA-Interim data for three sites. The interventions (indicated by red vertical lines) for ONSA and the first one at SPT0 are easily seen. In addition, the date of receiver changes are also shown in Figure 3 (indicated by green vertical lines) where no clear offsets are observed before and after each change. The impact of the receiver change was also examined by *Johansson et al.* (2002) where they performed a number of solutions with two different GPS receivers connecting to a same antenna and determined differences at the 1 mm level or less in coordinates ($\sim$0.05 kg/m^2 in IWV).

In order to carry out a correction on the GPS IWV time series for the offset caused by an intervention, a reference time period needs first to be chosen. Thereafter the estimated mean differences, relative to the reference time period, were applied to the other parts of the IWV time series. We investigated the impact of using different reference time period on resulting IWV means and trends after the offset corrections for three GPS sites with two interventions in their IWV time series. We found as expected that trends are not affected by which reference period that is chosen (the maximum difference is smaller than 0.01 kg/(m^2·decade)) but the overall mean differences compared to other techniques will. The differences in the overall means are shown in Table 3. A relatively large difference (1.4 kg/m^2) is seen from the site SPT0 when the last time period was used as the reference period. It is because this reference time period is short (less than 4 months). We decided to use the

time period that has the smallest offset relative to the ERA-Interim IWV and has a data length longer than 1 year as the reference period for the offset corrections of the GPS data.

Table 4 shows the mean and the standard deviation of the IWV difference between the radiosonde data and the GPS data before and after corrections for the GPS interventions. For three sites (ONSA, OLIK, and SPT0) the IWV mean difference change significantly after the offset correction is carried out on the GPS data. For other sites (JON0, METS, SKE0 and VAN0) the changes are insignificant. It seems as the change of radome type (ONSA and OLKI) and the addition of the microwave absorber at SPT0 have larger impacts than receiver and antenna changes. We note that the corrections for the interventions are derived from comparing GPS and ERA-Interim, but in Table 4 we compare the IWV from GPS with the radiosondes. Although radiosonde data are one of inputs to ERA-Interim, it is not granted that the correction shall have a positive impact.

3.2.2 Unknown interventions

After the corrections for all known interventions the site-related inconsistences, caused by hardware changes, were largely removed. In addition, in our GPS solutions the data-processing-related changes (i.e., interventions due to updates of the reference frame and applied models, implementation of a different elevation cutoff angle, different mapping functions, and other differences in the processing strategies) are eliminated by homogenously reprocessed data. Therefore, if there are any interventions left in the GPS data, it is mostly like due to changes in the electromagnetic environment caused by changing multipath effects. Additionally they can also be due to interventions in the reference data, in our case, ERA-Interim.

As pointed out by *Ning and Elgered* (2012), elevation-angle-dependent errors, e.g., signal multipath, including scattering, have a larger impact on the GPS observations acquired from lower elevation angles. We, therefore, decided to carry out a further assessment on the homogeneity of the GPS 10° solution using the PMTred test which was presented by *Ning et al.* (2016b). The time series of the IWV difference between the GPS 10° and the ERA-Interim data were used for the PMTred test. Three more interventions were detected (see Table 5) for three sites (SODA, OVE0, and OLKI). The resulting mean IWV differences vary from -0.74 to $+0.17$ kg/m^2.

4 Results

4.1 IWV comparison

Figure 4 and 5 depict comparisons of IWV estimates obtained from the different data sets for the entire 20 year long IWV time series. Note that one radiosonde site can be compared to multiple GPS sites. The offset corrections were applied to the GPS sites with known interventions (the ones given in Table 2), using the method discussed in Section 3.2. The corrections of the GPS 10° data with

unknown intervention (see Table 5) were not applied here, only for the trend comparisons and will be discussed in Section 4.3.

In general the mean IWV differences between two GPS solutions are below 1 kg/m^2 except the site of SODA which also has the largest mean differences when comparing the GPS 25° solution to the radiosonde and ERA-Interim data (see Figure 5). This is probably due to SODA is the most northern site in the investigated region and that snow on the antenna and its mount during the winters has an impact on the IWV estimates given by different GPS elevation cutoff angle solutions.

The comparisons show, as expected, that the standard deviation of the IWV difference increases as the distance between the GPS and the radiosonde sites becomes larger. This behaviour is not seen when ERA-Interim and GPS are compared possibly because the ERA-Interim IWV were interpolated horizontally to the location of the GPS site. In addition, the IWV difference between the GPS 25° elevation cutoff solution and the other two data sets gives a larger standard deviation than the corresponding ones obtained for the GPS 10° solution. This is due to larger formal errors of the individual IWV estimates caused by a worse satellite geometry and the reduced number of the observations when applying a higher elevation cutoff angle.

4.2 The relation between the ZTD and the IWV trends

Before presenting and comparing the estimated trends in the IWV it is appropriate to study possible trends in the parameters used in the conversion from the ZTD to the IWV according to Equations (1)–(5). All estimated trends are presented in Table 6. For all the sites the observed trends in the mean temperature, T_m, varies from 0.29 to 0.70 K/decade which correspond to 0.11 to 0.26 %/decade if we express the trends in percentage. These relative trends shall be compared to the relative trends in the IWV which range from 0.51 to 6.28 %/decade. Therefore, the IWV trends are approximately linearly related to the ZWD trends. Actually the correlation coefficient between the ZWD and the IWV trends is 0.9991. A strong correlation (0.94) is also seen between the ZTD and the ZWD (and to the IWV) trends.

The significance of the ZHD trends does not really matter since they are calculated accurately using measurements of the ground pressure. Therefore, they are not important when subtracted from the ZTD and hence have almost no impact on the accuracy of the ZWD and the IWV trends

4.3 IWV trend comparison

Before comparing the IWV trends obtained from the different data sets, we calculated the corresponding trend uncertainties for the GPS data from the two different elevation cutoff angle solutions shown in Figure 6. In the top panel the trend uncertainties were obtained using the formal error of the individual IWV estimates assuming a white noise behaviour. As a result the trend uncertainties obtained from the two solutions are very small ($\sim$0.015 kg/(m^2·decade) for the 25° solution and $\sim$0.005 kg/(m^2·decade) for the 10° solution) using a time period of 20 years. The larger uncertainty

seen for the 25° solution is simply due to the larger formal error for each IWV estimated. Over all GPS sites the 1-sigma formal errors of the IWV estimate are approximately 0.4 kg/m^2 for the 10° solution and 1 kg/m^2 for the 25° solution (*Ning and Elgered*, 2012).

However the trend uncertainty estimated by assuming a white noise behaviour only indicates how the estimated trend differs from what would be expected if there is no other errors, or deviations, in the IWV data compared to the model. Actually the estimated IWV trends have rather large uncertainties caused by the true short term variation (the natural variability of the weather) which is not described by the model, i.e., the deviations from the model are correlated in time. In order to calculate the trend uncertainty after taking these variations into account, we used a model presented by *Nilsson and Elgered* (2008). These uncertainties are shown in the bottom panel of Figure 6 where the two solutions with different elevation cutoff angles show similar values varying between 0.20 and 0.25 kg/(m^2·decade). This is expected since in this case the unmodelled true short term variation of the IWV, which are common for both GPS solutions, is dominating the trend uncertainty.

As described in Section 3 IWV trends were estimated using the GPS and the ERA-Interim data acquired, from the very same hour, as the launches of the radiosondes. In order to investigated possible impacts on the estimated trend due to the different launch time of radiosonde measurements. For a subset of the radiosonde stations, having launches at both 0 h and 12 h, we estimated two IWV trends, one for each launch time. The results indicate that the selection of launch time did not have significant impact on the trend comparison between the radiosonde and other data sets (two GPS solutions and ERA-Interim). However, we note differences in the trends themselves estimated at 0 h and 12 h. This calls for further studies that are outside the scope of this manuscript.

4.3.1 The trends for different elevation cutoff angles

As discussed before the IWV trends from the GPS data were estimated under three different scenarios, i.e., (1) no corrections for interventions, (2) corrections carried out for known interventions, and (3) corrections also carried for interventions detected for unknown reasons, by a PMTred test, for the GPS 10° solution. Thereafter the GPS-derived trends for the two solutions using different elevation cutoff angles were compared to the synchronised trends from the ERA-Interim and the radiosonde data. The results are summarized in Table 7.

Relatively large root-mean-square (RMS) differences ($>$ 0.25 kg/(m^2·decade)) and low correlations ($<$ 0.6) are seen for the comparisons when no corrections were carried out on the GPS data. After the corrections for the known interventions both on GPS 10° and 25° solutions, the largest improvement seen in RMS differences is from 0.20 kg/(m^2·decade) to 0.14 kg/(m^2·decade) which is significant with an approximate 67 % confidence level. The correlation coefficients of trends to both radiosonde and ERA-Interim data are improved significantly by approximately 60 % and 15 % for the GPS 25° solution and 10° solution, respectively. When corrections, for the unknown interven-

tions, were also applied, the correlation coefficients for the GPS 10° solution are further increased (> 0.77) when compared to the trends obtained from other data sets.

We also carried out the comparison of the IWV trends between two GPS solutions for the different scenarios and the results are shown in Table 8. After the corrections for the known interventions the trend correlation is improved significantly from 0.22 to 0.86 where the standard deviation (SD) of the trend differences is decreased from 0.37 to 0.12 kg/m^2. The best agreement is seen when a further correction applied on the GPS 10° data where the correlation coefficient and SD values are 0.91 and 0.10 kg/m^2, respectively.

The GPS-derived IWV trends, after corrections for the known interventions (scenario 2), and the trends from the ERA-Interim and the radiosonde data are presented in Table 9 where the estimated trends and the corresponding uncertainties (after taking the short term variation of the water vapour into account), are given before and after the plus-minus sign ($\pm$), respectively. An overall result is that all estimated trends are positive (except one with a very small negative value). The trends from the ERA-Interim show a smaller variation (from 0.07 to 0.53 kg/(m^2·decade)) compared to those from GPS and radiosonde data. It is clear that the estimated IWV trends are comparable to the trend uncertainties, varying from 0.20 to 0.26 kg/(m^2·decade), for all techniques. These similar values of the trend uncertainties are expected due to the fact that all data sets were acquired during the same time period. In addition, we observe that the trend differences between the GPS data and the radiosonde data show no clear correlation to the site separation.

Table 9 also presents the mean trends (from 0.33 to 0.39 kg/(m^2·decade)) and SD of the trends (from 0.11 to 0.23 kg/(m^2·decade)) over all sites. The values given by *Ning and Elgered* (2012) were 0.01, 0.05, and 0.03 kg/(m^2·decade) for the mean trends obtained for the GPS elevation 10° solution, the elevation 25° solution, and radiosondes with SD of 0.33, 0.41, and 0.44 kg/(m^2·decade), respectively. The larger spread of the trends (large SD values and small mean trends) obtained by *Ning and Elgered* (2012) is probably because of the shorter time period of the data (14 years) meaning that the trend shows more sensitivity to deviations from the model, especially in the beginning and in the end of the selected time series (*Nilsson and Elgered*, 2008).

Figure 7 depicts the scatter plot of the trend comparison between the GPS data and the reference time series while the comparison between the radiosonde and ERA-Interim is shown in Figure 8. As shown in figures when the GPS-derived IWV trends, after corrections for the known interventions, are compared to the radiosonde and ERA-Interim data, the agreement is similar to what is given from the comparison between the two reference data sets themselves.

4.3.2 The trends between weighting and non-weighting GPS solutions

We compared the GPS-derived IWV trends with and without an elevation dependent data weighting to the trends obtained from the radiosondes and ERA-Interim data. The RMS and correlations are presented in Table 10. No significant differences are seen for the GPS 10° solution while the agree-

ment of the trend become significantly worse when the weighting was applied for the GPS 25° solution. The RMS difference increase, by more than 40%, from 0.14 to 0.22 and 0.20 kg/(m^2·decade), respectively when compared to the radiosonde and ERA-interim data. The corresponding correlation coefficients decrease, by over 35%, from 0.77 to 0.56, and 0.80 to 0.59, respectively. Our interpretation is that the elevation weighting will only be useful when the observations have larger impacts from multipath effects using low elevation angles. For the observations acquired from higher elevation angles, 25° in our case, the multipath impact is expected to be small. As a result the elevation weighting will weaken the contribution of data points just above 25° and the geometry will be weakened even further.

5 Conclusions

We have processed 20 years of GPS data acquired from 13 GNSS sites in Sweden and Finland using the two different elevation cutoff angles of 10° and 25°. We also carried out the test assessing the impact of applying elevation-dependent weighting of the observations. The GPS-derived IWV were compared to the ones obtained from the radiosonde data at 7 nearby ($<$ 120 km) sites and the IWV given by the ERA-Interim data.

We show that due to the larger formal errors of the individual IWV estimates a larger standard deviation is seen for the individual estimates of the IWV difference between the GPS 25° elevation solution and the other two techniques. On the other hand the larger formal error of the individual IWV estimates is not the limiting factor for the uncertainty of the estimated IWV trends.

When comparing the trends obtained from the GPS elevation cutoff angle solutions at 25° and 10° with the trends obtained from the radiosonde data, a large disagreement in trends is seen when we ignore the interventions in the GPS data. The largest improvement is obtained when we apply the corrections on both GPS solutions for the interventions caused by known hardware changes (i.e., antenna, radome and microwave absorbing material). A slightly better agreement with the trends from other data sets, and between the two GPS solutions is seen after a further corrections on the GPS 10° data for the interventions detected by a PMTred test.

Moreover elevation dependent weighting gives significantly worse agreements when comparing trends for the GPS 25° solution.

The results show that using different elevation cutoff angles is a valuable diagnostic tool that can be used for validation purposes and detection of possible site problems, such as multipath impacts. When using the GPS data to monitor the long-term change in the IWV, e.g., as linear trends, it is recommended to apply at least two different elevation cutoff angles in the data processing. Ideally the IWV trends obtained from the two significantly different cutoff angle elevation solutions should be the same if there is no significant long-term changes in the multipath impacts, or any other elevation dependent phenomena that affects the observations.

Compared to our previous study (*Ning and Elgered*, 2012) we find that the estimated trends for the different sites are now more consistent. For the 25° elevation cutoff angle the mean and standard deviation are for the 20 years 0.37 and 0.21 kg/m^2 compared to 0.08 and 0.41 kg/m^2 for the 14 years of data. Both in this study and the previous one we find that for no site the estimated trend becomes significantly different from the radiosonde and ERA-Interim data when the 25° cutoff angle was used. It suggests that if there is a large difference in estimated trends from two different cutoff angles, the use of the result from the higher cutoff angle is more representative since systematic effects are less probable.

Acknowledgement. We would like to thank Stefan Heise for providing the ERA-Interim data. We also thank the National Land Survey of Finland for making the FinnRef GPS data available. The map in Figure 1 was produced using the Generic Mapping Tools (*Wessel and Smith*, 1998).

References

Baldysz, Z,, Grzegorz Nykiel, G., Figurski, M., and Araszkiewicz, A.: Assessment of the Impact of GNSS Processing Strategies on the Long-Term Parameters of 20 Years IWV Time Series, *Remote Sens.*, 10(4), 496, doi:10.3390/rs10040496., 2018.

Berrisford, P., Dee, D., Poli, P., Brugge, R., Fielding, K., Fuentes, M., Kållberg, P., Kobayashi, S., Uppala, S., and Simmons A.:The ERA-interim Archive Version 2.0, *ERA Report Series 1*, ECMWF, Shinfield Park, Reading (Oct. 2011), https://www.ecmwf.int/en/elibrary/8174-era-interim-archive-version-20, 2011.

Bertiger, W., Desai, S.D., Haines, B., Harvey, N., Moore, A.W., Owen, S., and Weiss, J.P.: Single receiver phase ambiguity resolution with GPS data, *J. Geod.*, 84:327–337, doi:10.1007/s00190-010-0371-9, 2010.

Bock, O., Willis, P., Wang, J., and Mears, C.: A high-quality, homogenized, global, long-term (1993–2008) DORIS precipitable water data set for climate monitoring and model verification, *J. Geophys. Res. Atmos.*, *119*, 7209–7230, doi:10.1002/2013JD021124, 2014.

Boehm, J., Werl, B. and Schuh, H.: Troposphere mapping functions for GPS and very long baseline interferometry from European Centre for Medium-Range Weather Forecasts operational analysis data, *J. Geophys. Res.*, 111, B02406, doi:10.1029/2005JB003629, 2006.

Ding, M.H.: A neural network model for predicting weighted mean temperature, *J. Geod.*, 92, 1187–1198, doi:10.1007/s00190-018-1114-6, 2018.

Dirksen, R.J., Sommer, M., Immler, F.J., Hurst, D.F., Kivi, R., and Vömel H.: Reference quality upper-air measurements: GRUAN data processing for the Vaisala RS92 radiosonde, *Atmos. Meas. Tech.*, 7, 4463–4490, doi:10.5194/amtd-7-4463-2014, 2014.

Heise, S., Dick, G., Gendt, G. et al.: Integrated water vapor from IGS ground-based GPS observations: initial results from a 5-min data set, *Ann. Geophys.*, *27*, 2851–2859, doi:10.5194/angeo-27-2851-2009, 2009.

Huber, S., and Kaniuth, K.: On the weighting of GPS phase observations in the EUREF network processing, *EUREF Symposium*, Toledo, Spain, June 4–7, 2003.

Jarlemark, P.O.J., Emardson, T.R., and Johansson, J.M.: Wet delay variability calculated from radiometric measurements and its role in space geodetic parameter estimation, *Radio Sci*, 33:719–730, doi:10.1029/98RS00551, 1998.

Johansson, J., Davis, J., Scherneck, H.G., Milne, G., Vermeer, M., Mitrovica, J., Bennett, R., Jonsson, B., Elgered, G., Elosegui, P., Koivula, H., Poutanen, M., Ronnang, B., and Shapiro, I.: Continous GPS measurements of postglacial adjustment in Fennoscandia 1. Geodetic result, *J. Geophys. Res.*, 107(B8):2157, doi: 10.1029/2001JB000400, 2002.

Larson, K.M., Braun, J.J., Small, E.E. et al.: GPS multipath and its relation to near-surface soil moisture content, *IEEE J-STARS*, *3*, 91–99, doi:10.1109/JSTARS.2009.2033612, 2010.

Lyard F., Lefevre, F., Letellier, T. et al.: Modelling the global ocean tides: Modern insights from FES2004, *Ocean Dyn.*, 56, 394, doi:10.1007/s10236-006-0086-x, 2006.

Nilsson, T. and Elgered, G.: Long-term trends in the atmospheric water vapor content estimated from ground-based GPS data, *J. Geophys. Res.*, 113, D19, D19101, doi:10. 1029/2008JD010110, 2008.

Ning, T., and Elgered, G.: Trends in the atmospheric water vapor content from ground-based GPS: the impact of the elevation cutoff angle, *IEEE J-STARS*, *5(3)*, 744–751, doi:10.1109/JSTARS.2012.2191392, 2012.

Ning, T., Haas, R., Elgered, G., and Willén, U.: Multi-technique comparisons of ten years of wet delay estimates on the west coast of Sweden, *J. Geod.*, 86(7), 565–575, doi:10.1007/s00190-011-0527-2, 2012.

Ning, T., Elgered, G., Willén, U., and Johansson, J. M.: Evaluation of the atmospheric water vapor content in a regional climate model using ground-based GPS measurements, J. Geophys. Res., 118, 329–339, doi:10.1029/2012JD018053, 2013.

Ning, T., Wang, J., Elgered, G. et al.: The uncertainty of the atmospheric integrated water vapour estimated from GNSS observations. *Atmos. Meas. Tech.*, 9, 79–92, doi:https://doi.org/10.5194/amt-9-79-2016, 2016a.

Ning T., Wickert, J., Deng, Z., Heise, S., Dick, G., Vey, S., and Schoene, T.: Homogenized Time Series of the Atmospheric Water Vapor Content Obtained from the GNSS Reprocessed Data, *J. Climate*, doi: 10.1175/JCLI-D-15-0158.1., 2016b.

Pacione, R., Araszkiewicz, A., Brockmann, E., and Dousa, J.: EPN-Repro2: A reference GNSS tropospheric data set over Europe, *Atmos. Meas. Tech.*, 10, 1,689–1,705, https://doi.org/10.5194/amt-10-1689-2017, 2017.

Parracho, A. C., Bock, O., and Bastin, S.: Global IWV trends and variability in atmospheric reanalyses and GPS observations, *Atmos. Chem. Phys.*, 18, 16,213–16,237, https://doi.org/10.5194/acp-18-16213-2018, 2018.

Pierdicca, N., Guerriero, L., Giusto, R. et al.: SAVERS: A Simulator of GNSS Reflections From Bare and Vegetated Soils, *IEEE Trans. Geosci. Remote Sensing*, *52(10)*, doi: 10.1109/TGRS.2013.2297572, 2014.

Saastamoinen, J.: Contributions to the theory of atmospheric refraction, *Bull Géod*, 107:13-34, doi:10.1007/BF02521844, 1973

Schmid, R., Steigenberger, P., Gendt, G., Ge, M., Rothacher, M.: Generation of a consistent absolute phase center correction model for GPS receiver and satellite antennas, *J. Geod.*, 81, 781–798, doi:10.1007/s00190-007-0148-y, 2007.

Schöne, T., Schön, N., and Thaller, D.: IGS Tide Gauge Benchmark Monitoring Pilot Project (TIGA)–Scientific Benefits, *J. Geod.*, 83, 249–261, doi:10.1007/s00190-008-0269-y, 2009.

Steigenberger, P., Tesmer, V., Krügel, M., Thaller, D., Schmid, R., Vey, S., and Rothacher, M.: Comparisons of homogeneously reprocessed GPS and VLBI long time-series of troposphere zenith delays and gradients, *J. Geod.*, *81(6-8)*, 503–514, doi:10.1007/s00190-006-0124-y, 2007.

Vey, S., Dietrich, R., Fritsche, M., Rülke, A., Steigenberger, P., and Rothacher, M.: On the homogeneity and interpretation of precipitable water time series derived from global GPS observations, *J. Geophys. Res.*, *114*, D10101, doi:10.1029/2008JD010415, 2009.

Vey, S., Dietrich, R., Rülke, A., Fritsche, M., Steigenberger, P., and Rothacher, M.: Validation of Precipitable Water Vapor within the NCEP/DOE Reanalysis Using Global GPS Observations from One Decade, J. Climate, 23, 1,675–1,695, doi:10.1175/2009JCLI2787.1, 2010.

Wang, J., Zhang, L., Dai, A., Hove, T.V., and Baelen, J.V., A near-global: 2-hourly data set of atmospheric precipitable water from ground-based GPS measurement, J. Geophys. Res., 112, doi: 10.1029/2006JD007529, 2007.

Webb, F.H. and Zumberge, J.F.: An Introduction to the GIPSY/OASIS-II. *JPL Publ.*, D-11088, Jet Propulsion Laboratory, Pasadena, California, 1993.

Wessel, P. and Smith, W.H.F.: New, improved version of generic mapping tools released, *EOS Trans. Amer. Geophys. U.*, 79, 47, 579, doi:10.1029/98EO00426, 1998.

WMO: Guide to Meteorological Instruments and Methods of Observation, 6th ed, WMO Rep. 8, World Meteorological Organization, Geneva, 1996.

Zumberge, J.F., Heflin, M.B., Jefferson, D.C. et al.: Precise Point Positioning for the Efficient and Robust Analysis of GPS Data from Large Networks, J. Geophys. Res., 102 (B3), 5005–5017, doi:10.1029/96JB03860., 1997.

Table 1. GPS sites and the nearby radiosonde sites, sorted by decreasing latitude.

GPS site		Long.	Lat.	Height[a]	RS site	Long.	Lat.	Height[a]	Distance	Height diff.
Acronym	Name	[°E]	[°N]	[m]	Name	[°E]	[°N]	[m]	[km]	[m]
SODA	Sodankylä	26.39	67.42	279	Sodankylä	26.65	67.37	158	12	121
OVE0	Överkalix	22.77	66.31	200	Luleå	22.13	65.55	−6	90	206
SKE0	Skellefteå	21.05	64.88	59	Luleå	22.13	65.55	−6	90	65
KIVE	Kivetty	25.70	62.82	198	Jyväskylä	25.67	62.40	114	47	84
SUN0	Sundsvall	17.66	62.23	7	Sundsvall	17.47	62.53	−20	35	27
OLKI	Olkiluoto	21.47	61.24	12	Jokioinen	23.50	60.82	84	119	−72
TUOR	Tuorla	22.44	60.42	41	Jokioinen	23.50	60.82	84	73	−43
METS	Metsähovi	24.40	60.22	76	Jokioinen	23.50	60.82	84	83	−8
VAN0	Vänersborg	12.07	58.69	135	Landvetter	12.30	57.67	119	114	16
JON0	Jönköping	14.06	57.75	227	Landvetter	12.30	57.67	119	105	108
SPT0	Borås	12.89	57.72	185	Landvetter	12.30	57.67	119	37	66
VIS0	Visby	18.37	57.65	55	Visby	18.35	57.65	20	1	35
ONSA	Onsala	11.93	57.40	9	Landvetter	12.30	57.67	119	37	−110

[a] The heights are referenced to the mean sea level.

Table 2. Known GPS site-related changes and the corresponding estimated mean IWV differences caused by the intervention.

Site	Date	Type of change	Mean difference for elevation 10° [kg/m^2]	Mean difference for elevation 25° [kg/m^2]
JON0	2002-08-23	Antenna	−0.16	−0.32
METS	2010-08-19	Antenna	0.29	−0.01
METS	2013-06-28	Antenna	−0.19	−0.22
ONSA	1999-02-02	Radome	0.63	−1.60
SKE0	2003-09-27	Antenna	−0.11	−0.04
SKE0	2008-03-14	Antennae	−0.27	−0.24
SPT0	2007-06-09	Absorber	−0.50	0.01
SPT0	2016-08-23	Antenna	−0.35	−1.40
VAN0	2003-03-30	Radome	−0.16	0.29
OLKI	2015-12-01	Radome	0.51	1.78

Table 3. Differences in IWV mean values due to different selections of the reference time period for intervention corrections

GPS site	Reference 1[a]	Reference 2[b]	Reference 3[c]	GPS [d]	ERA-Interim	Radiosonde
	[kg/m^2]	[kg/m^2]	[kg/m^2]	[kg/m^2]	[kg/m^2]	[kg/m^2]
Solution for an elevation cutoff angle at 10°						
METS	12.90	13.19	12.99	12.96	12.87	13.32
SKE0	11.70	11.59	11.32	11.59	11.40	12.14
SPT0	13.58	13.08	12.73	13.44	13.45	13.47
Solution for an elevation cutoff angle at 25°						
METS	13.11	13.12	12.91	13.08	12.87	13.32
SKE0	11.12	11.08	10.84	11.05	11.40	12.14
SPT0	12.02	12.04	10.62	12.00	13.45	13.47

[a]Use the first part of the time period without interventions as the reference.

[b]Use the middle part of the time period without interventions as the reference.

[c]Use the last part of the time period without interventions as the reference.

[d]The GPS mean value before the corrections for the interventions.

Table 4. The IWV comparison between radiosonde data and the GPS data before and after the corrections for the interventions in the GPS time series.

	Elevation 10° solution − Radiosonde			
	Before corrections		After corrections	
GPS site	Mean difference [kg/m^2]	Standard deviation [kg/m^2]	Mean difference [kg/m^2]	Standard deviation [kg/m^2]
JON0	−0.63	2.12	−0.55	2.11
METS	0.09	1.86	0.32	1.86
ONSA	0.40	1.62	0.55	1.60
SKE0	0.19	1.93	0.30	1.92
SPT0	−0.37	1.23	0.12	1.19
VAN0	−0.22	2.37	−0.14	2.36
OLKI	0.85	2.59	0.37	2.59
	Elevation 25° solution − Radiosonde			
JON0	−0.48	2.20	−0.32	2.20
METS	0.22	1.99	0.26	1.98
ONSA	0.16	1.81	−0.21	1.74
SKE0	−0.36	2.07	−0.28	2.06
SPT0	−1.43	1.38	−1.44	1.36
VAN0	−0.82	2.47	−0.96	2.46
OLKI	1.93	2.75	0.26	2.71

Table 5. The interventions detected by the PMTred test and the corresponding estimated mean IWV differences caused by the intervention for the GPS 10° solution. The GPS data (10° solution in this case) were first corrected for the known interventions (see Table 2), and then used for a PMTred test.

Site	Date	PTmax (CV)[a]	Mean difference for elevation 10° [kg/m^2]
SODA	2006-10	6.08 (5.94)	−0.28
OVE0	2005-06	6.48 (5.94)	0.17
OLKI	2013-05	15.96 (6.13)	−0.74

[a]The PTmax is the PMTred test statistic, while the corresponding critical value (CV), for a confidence level of 99.9 %, is given in the parenthesis. See details in *Ning et al.* (2016b)

Table 6. The IWV trends from the GPS elevation 10° and the trends in parameters used in the conversion from the ZTD to the IWV. The sites are sorted by decreasing latitude.

GPS site	ZTD [mm/decade]	ZHD [mm/decade]	Pressure P_0 [hPa/decade]	ZWD [mm/decade]	Mean temperature T_m [K/decade]	IWV [kg/(m^2·decade)]
SODA	2.99	0.06	0.03	2.93	0.53	0.45
OVE0	2.82	1.65	0.73	1.16	0.70	0.20
SKE0	3.66	1.83	0.81	1.82	0.50	0.29
KIVE	2.47	0.77	0.34	1.70	0.52	0.27
SUN0	2.48	1.42	0.63	1.05	0.43	0.18
OLKI	7.97	1.98	0.87	5.99	0.47	0.95
TUOR	5.21	2.00	0.88	3.21	0.59	0.53
METS	4.72	2.19	0.96	2.53	0.52	0.41
VAN0	2.88	1.16	0.51	1.71	0.35	0.28
JON0	2.86	1.47	0.65	1.39	0.31	0.23
VIS0	1.89	1.48	0.65	0.42	0.32	0.07
SPT0	2.38	1.39	0.61	0.99	0.32	0.17
ONSA	2.39	1.12	0.49	1.27	0.29	0.21

Table 7. Root-mean-square (RMS) differences and correlations (presented in parenthesis) between the trends obtained from the GPS solutions and the ones given by the radiosonde and the ERA-Interim data.

	Radiosonde			ERA-Interim		
	Difference 1[a]	Difference 2[b]	Difference 3[c]	Difference 1[a]	Difference 2[b]	Difference 3[c]
GPS 10°	0.25 (0.59)	0.18 (0.69)	0.15 (0.87)	0.25 (0.44)	0.20 (0.50)	0.10 (0.77)
GPS 25°	0.31 (0.46)	0.14 (0.77)	0.14 (0.77)	0.29 (0.50)	0.14 (0.80)	0.14 (0.80)

[a]No corrections in the GPS time series.

[b]GPS data were corrected for all known interventions (see Table 2) for both 10° and 25° solutions.

[c]GPS data were corrected, only for the 10° solution, for the interventions detected by the PMTred test (see Table 5).

Table 8. The trend difference between the GPS 10° and 25° solutions over all GPS sites.

	Difference 1[a]	Difference 2[b]	Difference 3[c]
Mean	0.02	−0.04	−0.08
Standard deviation	0.37	0.12	0.10
Correlation	0.22	0.86	0.91

[a]No corrections in the GPS time series.

[b]GPS data were corrected for all known interventions (see Table 2) for both 10° and 25° solutions.

[c]GPS data were corrected, only for the 10° solution, for the interventions detected by the PMTred test (see Table 5).

Table 9. The estimated IWV trends from all data sets after the correction on the GPS IWV data for all known interventions.

GPS site	Radiosonde site	Distance [km]	Number of paired observations	Trend [kg/(m^2·decade)]			
				GPS 10°	GPS 25°	Radiosonde	ERA-Interim
VIS0	Visby	1	11007	0.07±0.24	−0.05±0.24	0.08±0.25	0.07±0.23
SODA	Sodankylä	12	10756	0.45±0.21	0.50±0.23	0.29±0.22	0.34±0.21
SUN0	Sundsvall	35	15338	0.18±0.23	0.22±0.23	0.40±0.24	0.30±0.23
SPT0	Landvetter	37	11436	0.17±0.23	0.25±0.23	0.32±0.24	0.30±0.23
ONSA	Landvetter	37	11420	0.21±0.25	0.23±0.26	0.32±0.24	0.34±0.24
KIVE	Jyväskylä	47	9947	0.27±0.22	0.28±0.23	0.10±0.23	0.26±0.22
TUOR	Jokioinen	73	11644	0.53±0.26	0.66±0.26	0.79±0.25	0.53±0.25
METS	Jokioinen	83	12366	0.41±0.24	0.40±0.24	0.65±0.24	0.44±0.24
OVE0	Luleå	90	10805	0.20±0.20	0.50±0.20	0.41±0.23	0.44±0.20
SKE0	Luleå	90	10926	0.29±0.23	0.37±0.23	0.42±0.23	0.40±0.23
JON0	Landvetter	105	11636	0.23±0.23	0.24±0.23	0.31±0.24	0.28±0.23
VAN0	Landvetter	114	11584	0.28±0.23	0.40±0.24	0.33±0.24	0.33±0.23
OLKI	Jokioinen	119	10655	0.95±0.26	0.78±0.26	0.68±0.25	0.38±0.25
Mean trend				0.33	0.37	0.39	0.34
Standard deviation				0.23	0.21	0.21	0.11

Table 10. Root-mean-square (RMS) difference and correlations (presented in parenthesis), in comparison with the radiosonde and ERA-Interim data, between the GPS solutions with and without weighting.

	Radiosonde		ERA-Interim	
	Weighting	No weighting	Weighting	No weighting
GPS 10°[a]	0.19 (0.67)	0.18 (0.69)	0.20 (0.53)	0.20 (0.50)
GPS 25°[a]	0.22 (0.56)	0.14 (0.77)	0.20 (0.59)	0.14 (0.80)

[a]GPS data were corrected for all known interventions (see Table 2) for both 10° and 25° solutions.

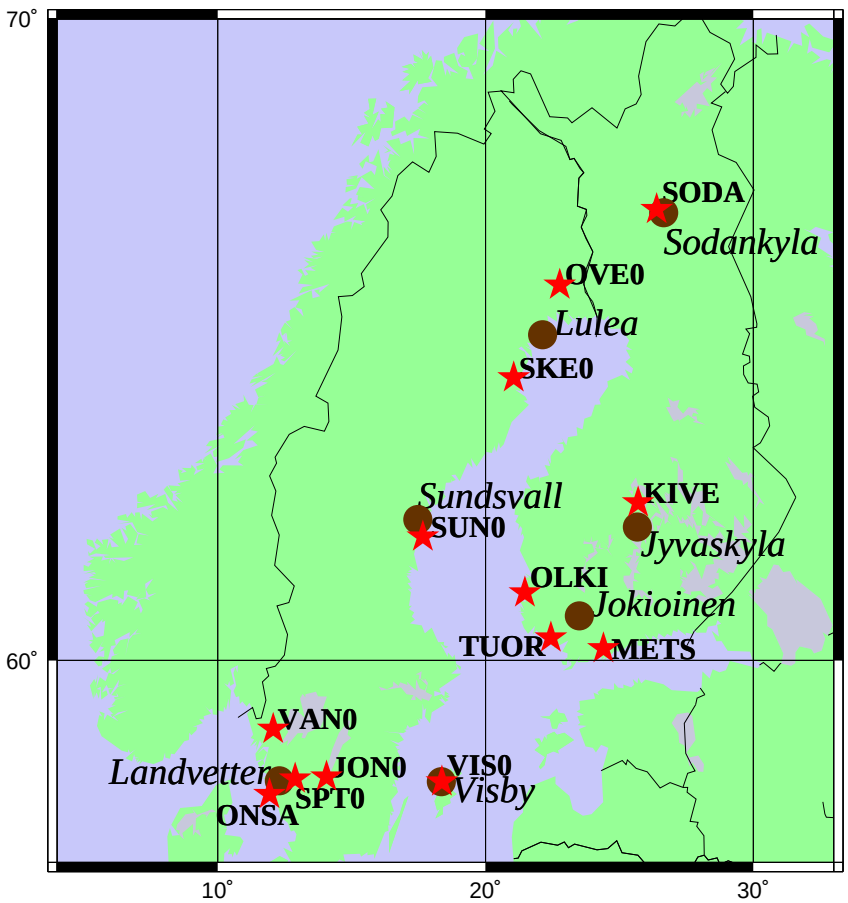

Figure 1. The 13 GPS sites (red stars) and the 7 radiosonde sites (brown dots).

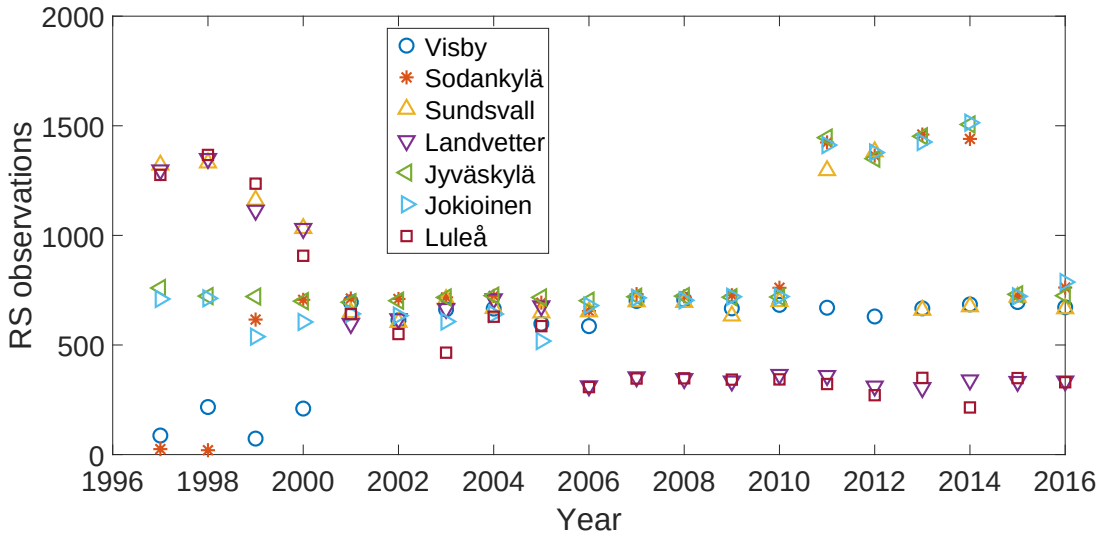

Figure 2. The number of radiosonde launches per year.

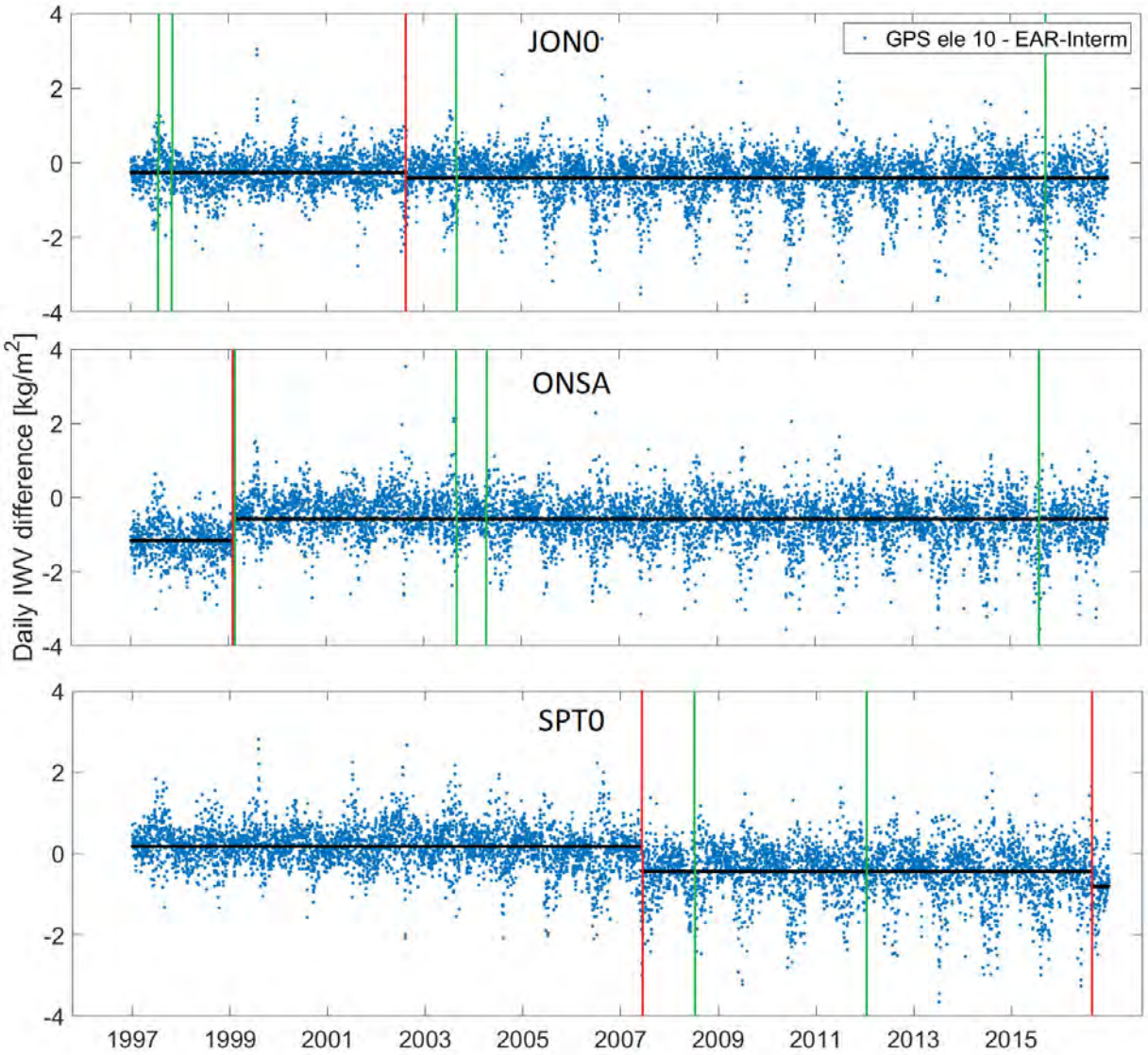

Figure 3. Time series of the daily mean IWV difference (GPS – ERA-Interim) for three sites: JON0, ONSA, and SPT0. Dark lines are the mean of IWV difference, red vertical lines indicate the date of the interventions (antenna and radome changes) and green vertical lines indicate the date of receiver changes.

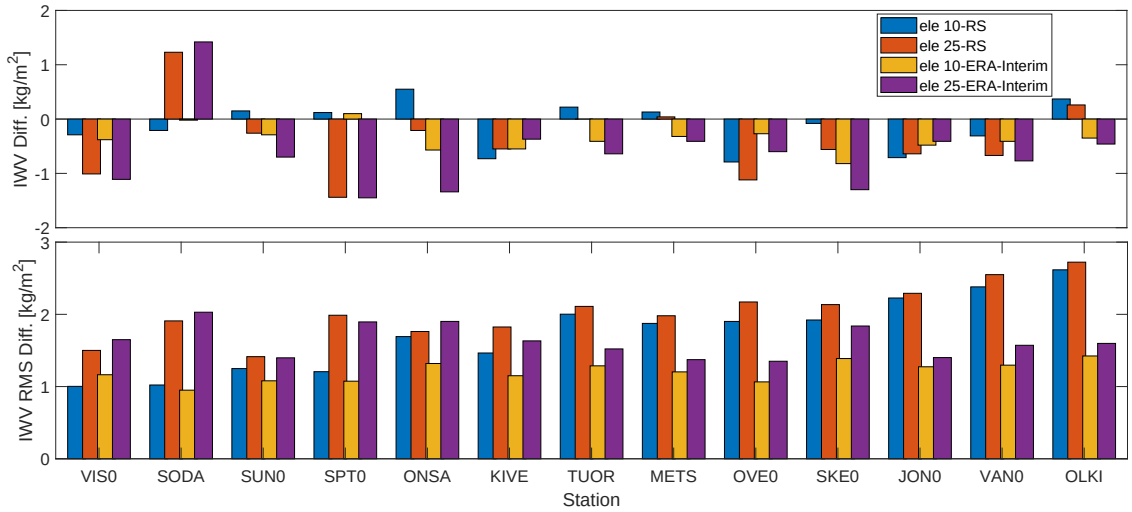

Figure 4. The mean (top) and the root-mean-square (bottom) of the IWV differences for the two different elevation cutoff angles. The GPS sites (from left to right) are sorted by increasing distance to the radiosonde site.

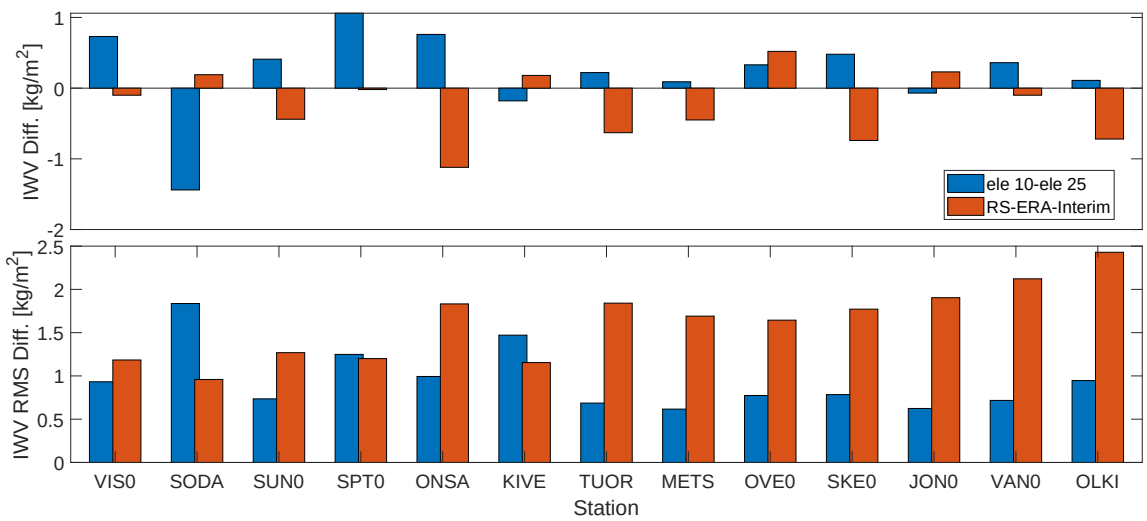

Figure 5. The mean (top) and the root-mean-square (bottom) of the IWV differences between two different GPS solutions, and between the radiosonde and the ERA-Interim data.

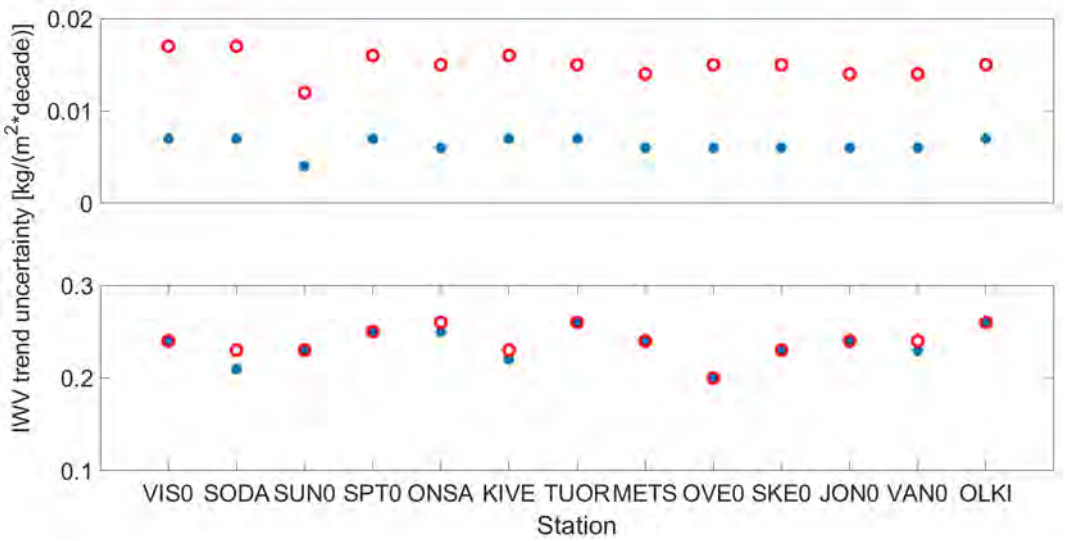

Figure 6. The uncertainties of the IWV trends obtained using the formal error of the GPS estimates and assuming a white noise behaviour (top), and after rescaling and taking the temporal correlation of the IWV into account (bottom). Open red circles and filled blue circles denote an elevation cutoff angle of 25° and 10°, respectively.

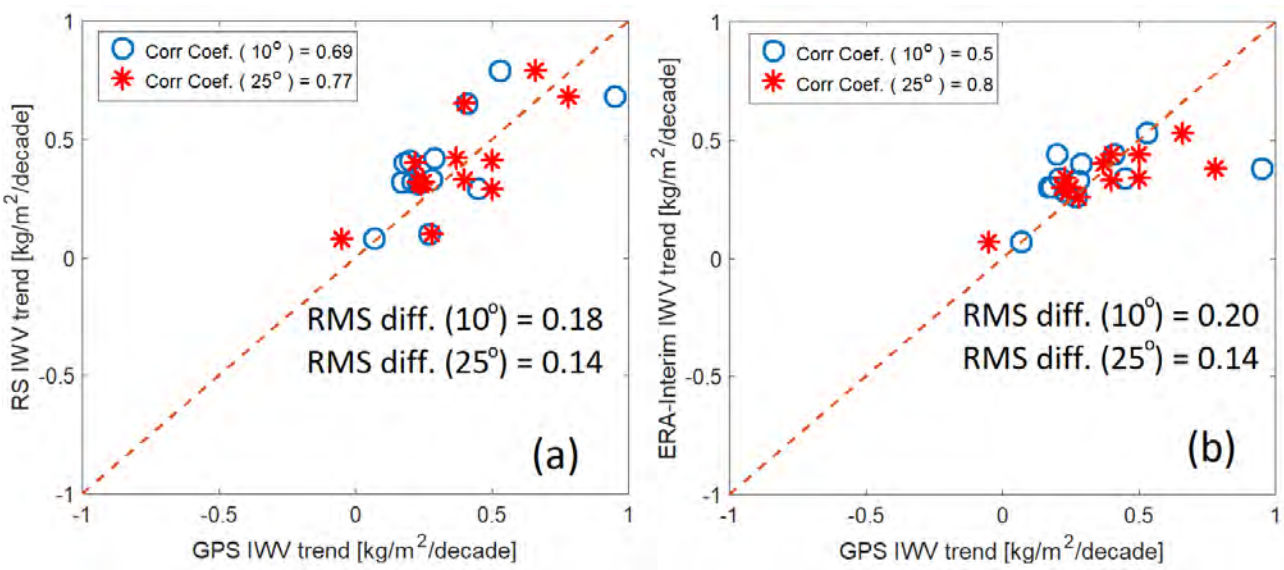

Figure 7. Correlations between the IWV trends from the GPS and the radiosonde (RS) data (a), and the ERA-Interim data (b) for 10° and 25° elevation cutoff angles after the correction on the GPS IWV data for all known interventions. The dashed lines show the perfect agreement.

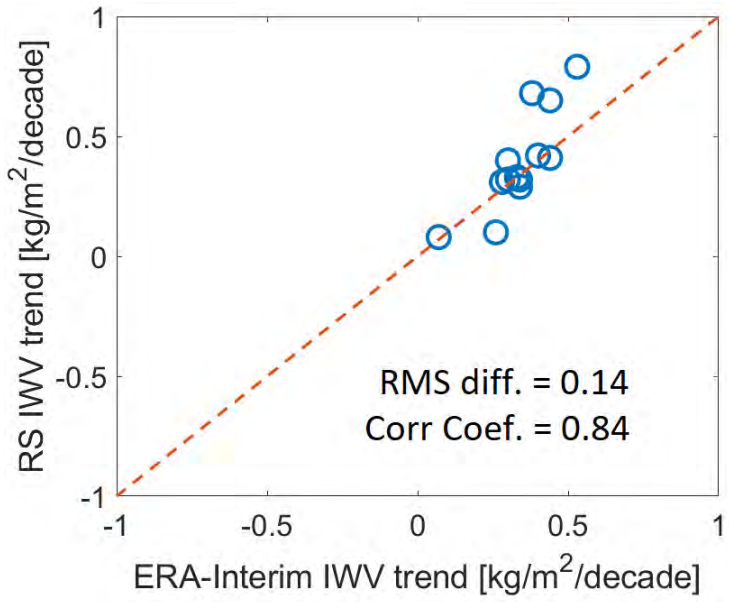

Figure 8. Correlations between the IWV trends from the radiosonde (RS) data and the ERA-Interim data.